ACS SyntheticBiology

Research Article

pubs.acs.org/synthbio

Automated Design of Genetic Toggle Switches with Predetermined Bistability

Shuobing Chen,[†,‡,∥] Haoqian Zhang,[†,‡,∥] Handuo Shi,[†,‡] Weiyue Ji,[†] Jingchen Feng,[†] Yan Gong,[†] Zhenglin Yang,[†] and Qi Ouyang*[,‡,§]

[†]Peking University Team for the International Genetically Engineered Machine Competition (iGEM), [‡]Center for Quantitative Biology and Peking-Tsinghua Center for Life Sciences, and [§]The State Key Laboratory for Artificial Microstructures and Mesoscopic Physics, School of Physics, Peking University, Beijng, 100871, China

Supporting Information

ABSTRACT: Synthetic biology aims to rationally construct biological devices with required functionalities. Methods that automate the design of genetic devices without post-hoc adjustment are therefore highly desired. Here we provide a method to predictably design genetic toggle switches with predetermined bistability. To accomplish this task, a biophysical model that links ribosome binding site (RBS) DNA sequence to toggle switch bistability was first developed by integrating a stochastic model with RBS design method. Then, to parametrize the model, a library of genetic toggle switch mutants was experimentally built, followed by establishing the equivalence between RBS DNA sequences and switch bistability. To test this equivalence, RBS nucleotide sequences for different specified bistabilities were *in silico* designed and experimentally verified. Results show that the deciphered equivalence is highly predictive for the toggle switch design with predetermined bistability. This method can be generalized to quantitative design of other probabilistic genetic devices in synthetic biology.

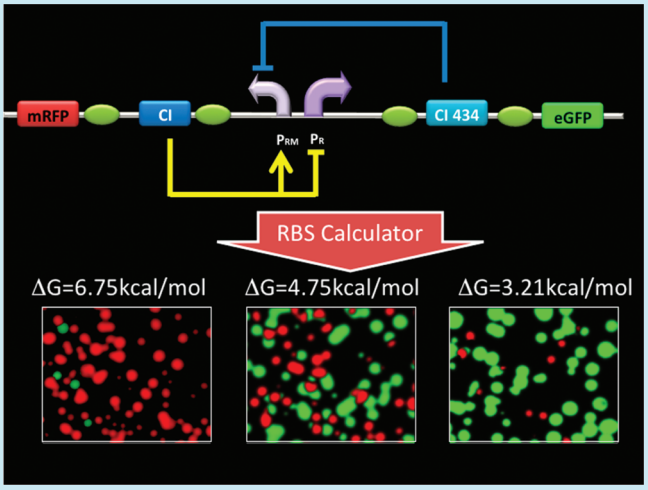

KEYWORDS: *genetic toggle switch, RBS calculator, rational design, stochastic model*

The goal of synthetic biology is to rationally build synthetic biological circuits with desired functionalities.[1] Since the genetic toggle switch[2] and the repressilator,[3] two landmarks in synthetic biology, significant progress in this line of research has been made. Genetic devices with a wide range of functionalities have been created,[4] for example, genetic switches,[5−7] oscillators,[8−11] and Boolean logic processors.[12−14] Despite this progress, however, some tremendous challenges still remain, one of which is how to rationally build genetic devices with predetermined performance.[4,15]

Among the most commonly used genetic devices in the functional circuit design is the toggle switch.[2,7,15] The genetic toggle switch is of great importance both in nature[16] and in artificial synthetic biology circuit[15] due to its bistability. This property not only confers cells the ability to stochastically switch between phenotypic states to generate diversity in a population[17,18] but also makes the toggle switch the core component of gene circuits for higher-level sequential logic processes, such as adaptive learning.[2,7,15] We previously constructed a robust genetic toggle switch using phage repressors cI and cI434;[7] the fine-tuning of the switch bistability, however, still needs the building of large component libraries, such as a ribosome binding site (RBS) mutant library, followed by individual characterization and modeling, which is laborious and time-consuming.[4,7,15,19] Moreover, this process probably needs to be repeated case by case during gene circuit construction, because of different requirements toward the switch bistability for module assembly.

Therefore, there is a pressing need to develop methods to rationally design genetic devices with predetermined characteristics.[15,20] Recently, studies have shown that biological process can be quantitatively modeled and reliably predicted if integrated modeling is undertaken.[21−23] Salis et al. have developed a thermodynamic model to quantify translation strength of RBS in bacteria.[23] Software derived from this model, called the RBS calculator, can be used to both rationally forward-engineer RBS sequences with predetermined translation strength and quantitatively predict translation strengths of different RBS sequences for a given protein coding

Special Issue: Synthetic Biology: Research Perspectives from China

Received: April 5, 2012
Published: May 4, 2012

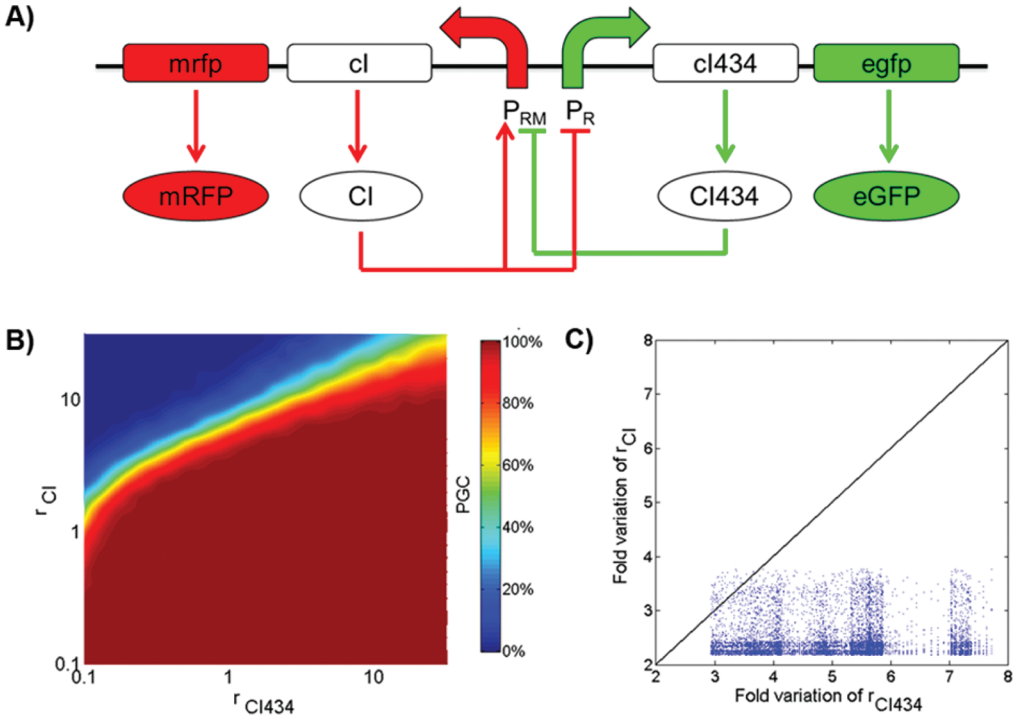

Figure 1. Bistable distribution of cell population as a function of translation strength of CI434 and CI. (A) Detailed schematic of genetic toggle switch used in this work. Rectangles and ovals represent genes and their translated proteins, respectively. Solid lines with arrows indicate regulating relations between genes, with sharp ones representing activation and blunt ones repression. (B) Simulation results showing bistable distribution of cell population as a function of r_{CI} and r_{CI434}. Different colors show diverse PGC values, as indicated by color bar on the right. The colorful band from bottom left to top right is the transition interval from PGC ≈ 100% (dark red region) to PGC ≈ 0% (blue region). (C) Fold variations of r_{CI} and r_{CI434} across the bistability transition interval calculated from 10,000 different toggle switches *in silico*. Shown here is one representative of three independent simulation results. See the calculation method shown in Supplementary Figure S1. Larger fold variation of r_{CI} or r_{CI434} is equivalent to wider respective transition interval. Each point represents a set of fold variations of r_{CI} and r_{CI434} for a specific toggle switch. Black line stands for $r_{CI} = r_{CI434}$.

sequence.[23] It has been regarded as a powerful tool to help the rational design of genetic devices.[1,15,19]

Here we provide a method for rational design of genetic toggle switches with predetermined bistability. A stochastic model was first constructed to guide the experimental implementation of bistability tuning. By integrating the stochastic model with the RBS design method, the relationship (equivalence) between the RBS DNA sequence of cI434 and the toggle switch bistability was then established. A library of genetic toggle switches with different RBS sequences prefixing cI434 was then experimentally built. We analyzed the mutation library and parametrized the equivalence. With this equivalence, RBS nucleotide sequences predicted for different specified switch bistability were *in silico* designed and experimentally verified. Our experimental results demonstrate that this method could be very predictive and extensible for the rational design of genetic toggle switches.

In this research, the genetic toggle switch mainly consists of a positive feedback loop and a double-negative feedback loop[7] (Figure 1A). The promoters P_R and P_{RM} control, respectively, the expression of two mutually repressed repressors, CI434 and CI. In addition, CI can activate promoter P_{RM}, which reinforces the bistable behavior by increasing the bistability robustness of the circuit.[7] Green fluorescence protein (EGFP) and red fluorescence protein (mRFP) were, respectively, adopted as indicators of CI or CI434 expression dominance within a cell (Figure1A). Intuitively, modulating the translation strength of CI (r_{CI}) or CI434 (r_{CI434}) and thereby the repression balance between cI and cI434 could tune the switch bistability. To quantitatively address this tuning effect, we constructed a set of ordinary differential equations (ODEs), based on which a stochastic model was further built to simulate its kinetic dynamics (see Supporting Information). With reasonable parameter sets (Supplementary Table S4), a cell population was simulated *in silico*, and the bistable distribution of this cell population as function of r_{CI434} and r_{CI} strength was recorded. Our computer simulation showed that at the asymptotic state (after a long period of reaction time) the proportion of GFP-dominant cells (PGC) was mainly determined by the value of r_{CI434} and r_{CI} only, and regardless of initial states (see Supporting Information). Figure 1B provides the bistable distribution of cell population as a function of r_{CI} and r_{CI434}. When r_{CI} is small but r_{CI434} is large, population tends to be CI434-dominant (i.e., GFP-dominant), and thereby PGC tends to be nearly 100%, whereas with large r_{CI} but small r_{CI434}, most cells would be CI-dominant (i.e., RFP-dominant), and PGC would be quite close to 0% (Figure 1B).

In order to make later experimental quantification easier, we took PGC as an index to describe switch bistability. PGC is a function of r_{CI434} and r_{CI}, as shown in eq 1 (see the detailed mathematical derivation in Supporting Information):

$$\mathrm{PGC} = f(r_{CI434}, r_{CI}) \tag{1}$$

The quantitative relationship between r_{CI434} and switch bistability (PGC) can thus be established in later simulation.

Two characteristics stand out in Figure 1B: the asymmetric response of PGC to r_{CI} and r_{CI434} and the narrow bistability

dx.doi.org/10.1021/sb300027y | ACS Synth. Biol. 2012, 1, 284–290

transition interval. The first characteristic is mainly due to asymmetric circuit topology (see Supporting Information), which does not cause any difficulty in circuit design; the second, however, warrants special concern. One observes that the transition interval from large PGC (≈100%) to small PGC (≈0%), a parameter space region where diverse bistable distribution exists, is quite narrow (although "wide" enough compared with other topologies taken previously[7]). Therefore, we need to investigate a way to fine-tune the control parameters within such a sharp interval for the system in order to predetermine bistable state (i.e., predetermined PGC).

Reasonably, within the bistability transition interval (Figure 1B), the larger fold the control parameter (r_{CI} or r_{CI434}) could change over, the more meticulously the bistability could be tuned. We thus need to select a more tunable parameter between the two. For this purpose, we simulated 10,000 toggle switches (with different sets of r_{CI} and r_{CI}) randomly adopted from Figure 1B and calculated fold variation of r_{CI434} and r_{CI} across the bistability transition interval by varying r_{CI} and r_{CI434}, respectively (larger fold variation of r_{CI} or r_{CI434} indicates wider respective transition interval). As an example shown in Supplementary Figure S1, when r_{CI} was fixed, the fold variation of r_{CI434} was 5.0 for PGC to vary from 10% to 90%; when r_{CI434} was fixed, the fold variation of r_{CI} was 3.1 for the same purpose. Simulation was independently performed three times. For each simulation, all sets of fold variations of r_{CI} and r_{CI434} calculated were plotted (Figure 1C, Supplementary Figure S2). Most points (>99% throughout all three sets of simulation results) locate below the line corresponding $r_{CI} = r_{CI434}$, indicating that the fold variation of r_{CI434} is much larger than that of r_{CI} in most cases. We concluded that control parameter r_{CI434} permits a wider transition interval. Besides, considering the possible error of experimental implementation, the effect of tuning r_{CI} will be unpredictable due to its narrow bistability transition interval. Therefore, we decided to use r_{CI434} as the control parameter for bistability fine-tuning.

We then fixed r_{CI} as a constant, and as a result PGC presented as the function of r_{CI434} only (Supplementary Discussion):

$$\mathrm{PGC} = f(r_{CI434}) \tag{2}$$

Accordingly, cell population distribution as a function of r_{CI434} for 1000 cells was simulated. As expected, r_{CI434} smoothly affects the bistable distribution of cell population: the larger r_{CI434} is, the larger PGC (Figure 2) represents. For instance, three distinct values of r_{CI434} (0.15, 0.70, and 1.05 au) resulted in different bistable distributions of cell population (PGC of 8.7%, 50.4%, and 93.2%, respectively). The variation fold of r_{CI434} within the bistability transition interval (PGC from 10% to 90%) is 40 (Figure 2). As a control, similar simulation on cell population distribution as a function of r_{CI} was also performed, the result of which was a variation of 2 fold (Supplementary Figure S3).

The next task is to establish the relationship between r_{CI434} and the RBS DNA sequence. For any specific mRNA sequence of cI434, we could calculate the difference of Gibbs free energy between the folded nascent mRNA transcript state and the assembled 30S pre-initiation complex state, ΔG_{CI434}, using the RBS calculator (Figure 4A). In an equilibrium statistical thermodynamic model based on Salis et al.,[23] r_{CI434} could be quantified through eq 3:

$$r_{CI434} = K_{CI434}\, e^{-\beta \Delta G_{CI434}} \tag{3}$$

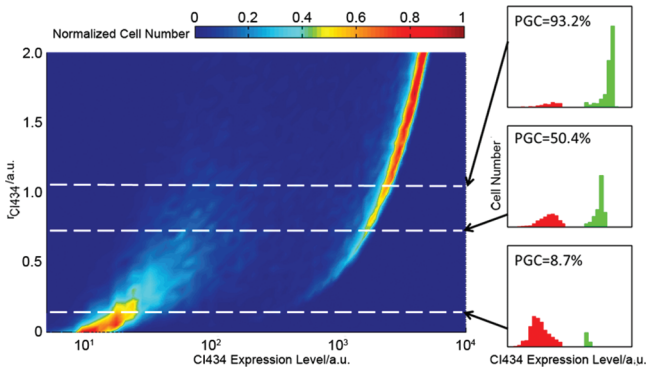

Figure 2. The proportion of GFP-dominant cell (PGC) within a cell population is smoothly affected by translation strength of CI434. In the left panel, the horizontal axis denotes CI434 expression level while the vertical axis represents r_{CI434}. Different colors stand for normalized cell density, as indicated by the color bar at the top. With increasing r_{CI434}, distribution of cell population smoothly transits from CI-dominant state (RFP-dominant state, with expression level of CI434 around 10 au) to CI434-dominant state (GFP-dominant state, with expression level of CI434 higher than 10^3 au). When r_{CI434} is small, cells tend to highly express CI, as represented by the dashed line at the bottom (left panel), where PGC is 8.7% (right panel). With a fairly large r_{CI434}, some cells show a RFP-dominant state while others show GFP-dominance, indicated by the dashed line in the middle (left panel), and its corresponding PGC is 50.4% (right panel). When r_{CI434} is large enough, most cells would be CI434-dominant, as the top dashed line (left panel) and subfigure represents, with a PGC of 93.2% (right panel).

where β is the apparent Boltzmann constant, and constant K_{CI434} depends on factors independent of CI434 translation initiation. Equation 3 predicts a linear relationship between ln r_{CI434} and ΔG_{CI434}, which could be transformed as

$$\ln r_{CI434} = -\beta \Delta G_{CI434} + \ln K_{CI434} \tag{4}$$

By integrating the stochastic model (eq 2) with the RBS calculator (eq 4), it was expected that the values of K_{CI434} and β could be specified through r_{CI434} (solved from PGC) and ΔG_{CI434} (calculated from RBS DNA sequence). Thus the equivalence relationship between cI434 RBS DNA sequence and switch bistability (PGC) was established. We next sought to experimentally address it.

Using the construction flow developed previously,[7] an original version of cI-cI434 toggle switch was constructed and then cloned into pSB1C3 plasmid backbone via standard assembly.[24] In order to modulate r_{CI434}, directed mutagenesis was performed (the detailed sequence feature of the original toggle switch is shown in Supporting Material). Degenerate primers were used to introduce random mutations at the RBS sequence prefixing the cI434 coding sequence (Supplementary Figure S4A). Together with the original switch, 69 resulted mutants were randomly selected for the following characterization (regarded as 70 mutants later on). Each switch mutant was then transformed into *E. coli.* DH5α cells, followed by overnight growth under 37 °C and overnight storage under 4 °C to accumulate enough fluorescence proteins.

We statistically examined PGC, the bistability index, of all 70 toggle switch mutants on agar plates via a convenient scoring method. For a colony expressing RFP only, its score is 0, and for a colony expressing GFP only, its score is 1. As for a "mosaic colony", it was scored according to the surface proportion of GFP-expressing section (Supplementary Figure S7). The

dx.doi.org/10.1021/sb300027y | *ACS Synth. Biol.* 2012, 1, 284–290

Figure 3. Mutation libraries of RBS sequences prefixing cI434 and cI. (A) All selected toggle switch mutants from mutagenesis at cI434-RBS. 20 mutants out of 70 show PGC value ranging from 2% to 98%. (B) All selected toggle switch mutants from mutagenesis at cI-RBS. Note that compared with panel A, among 36 toggle switch mutants only 1 shows a PGC value within 2−98%.

mosaic colonies denote colonies whose expression of fluorescence reporters was not overlapping but sectored (Supplementary Figure S6). This phenomenon was also observed previously;[7] it could be attributed to the stochastic establishment of different stable states during early stage growth of colony. The resulted sum score of each selected region was normalized by the total number of colonies scored in a region, derived as a relative score, the required PGC. Results showed that, for 20 mutants out of 70, their PGC values locate within a range of 2−98%. Especially, 6 of them fell into the range of PGC from10% to 90%, the significant bistability transition interval (Figure 3A, Figure 4B, Supplementary Table S1).

Serving as control, mutagenesis was also performed at RBS-cI sequence of the original toggle switch (Supplementary Figure S4B). Using the same treatment as above, 36 toggle switch mutants were selected and characterized. Reassuringly, among 36 mutants, only one mutant's PGC value locates within 2−98% (Figure 3B, Supplementary Table S3). All other mutant toggle switches result in either PGC = 100% (all colonies are green) or PGC = 0% (all colonies are red). The mutation results support our modeling conclusion that r_{CI434} tunes the switch bistability much more meticulously than r_{CI} because of the larger variation fold of r_{CI434} within bistability transition interval.

To precisely parametrize β and constant K_{CI434} in eq 4, RBS-cI434 mutants whose PGC values ranged from 10% to 90% were selected and sequenced (Table 1). Acquired RBS sequences were exploited to predict the Gibbs free energy change of translation initiation (ΔG_{CI434}) using online RBS Calculator v1.1 (Figure 4A). Calculated ΔG_{CI434} of these RBS mutants ranged from 0.75 kcal/mol (the strongest) to 6.75 kcal/mol (the weakest) (Table 1, Figure 4B). Then, using the information from numerical simulation (Figure 2), the r_{CI434} value was evaluated for the selected RBS mutants that have different values of PGC. Thereby, constant K_{CI434} and apparent Boltzmann constant β can be parametrized by linear regression between ln r_{CI434} and ΔG_{CI434} based on eq 4 (inset in Figure 5). In this way, the value of ln K_{CI434} was evaluated to be 2.21 ± 0.06 (R^2 = 0.997), and β value was measured to be 0.50 ± 0.01 mol/kcal. With evaluated constant K_{CI434} and β, an equivalence curve relating ΔG_{CI434} of cI434 RBS to switch bistability (PGC) was thereby parametrized according to eqs 4 and 2 (Figure 5, Supplementary Discussion).

Beside predicting r_{CI434} for given RBS sequences, RBS Calculator can also automatically design RBS sequences to

Table 1. Sequences and Statistics of cI434 RBS Mutants

no.	RBS sequences	ΔG (kcal/mol)	PGC (%)
RBS-cI434 Library Mutants Used for Parametrization			
C01	5′-**TTTATGT**GGTTGT**ATG**-3′	5.65	21 ± 7
C42	5′-**CGAGACC**GGTTGT**ATG**-3′	3.21	90.9 ± 0.8
C68	5′-**CTTCCGT**GGTTGT**ATG**-3′	4.75	60 ± 2
C77	5′-**AGACAAC**GGTTGT**ATG**-3′	6.75	8 ± 2
E07	5′-**CCAAAAC**GGTTGT**ATG**-3′	3.35	88 ± 1
E06	5′-**CCTAACC**GGTTGT**ATG**-3′	4.35	64 ± 5
In silico Designed cI434 RBSs Using the Equivalence Curve			
F01	5′-**ACAACCC**GGTTGT**ATG**-3′	8.05	0
F02	5′-**ATACTTC**GGTTGT**ATG**-3′	6.65	1.0 ± 0.3
F03	5′-**CCTAGGC**GGTTGT**ATG**-3′	4.55	42 ± 5
F04	5′-**CCGCCGA**GGTTGT**ATG**-3′	3.65	87 ± 5
F05	5′-**AATACGA**GGTTGT**ATG**-3′	2.15	99.1 + 0.4
F06	5′-**CATCAGA**GGTTGT**ATG**-3′	0.75	100

dx.doi.org/10.1021/sb300027y | *ACS Synth. Biol.* 2012, 1, 284−290

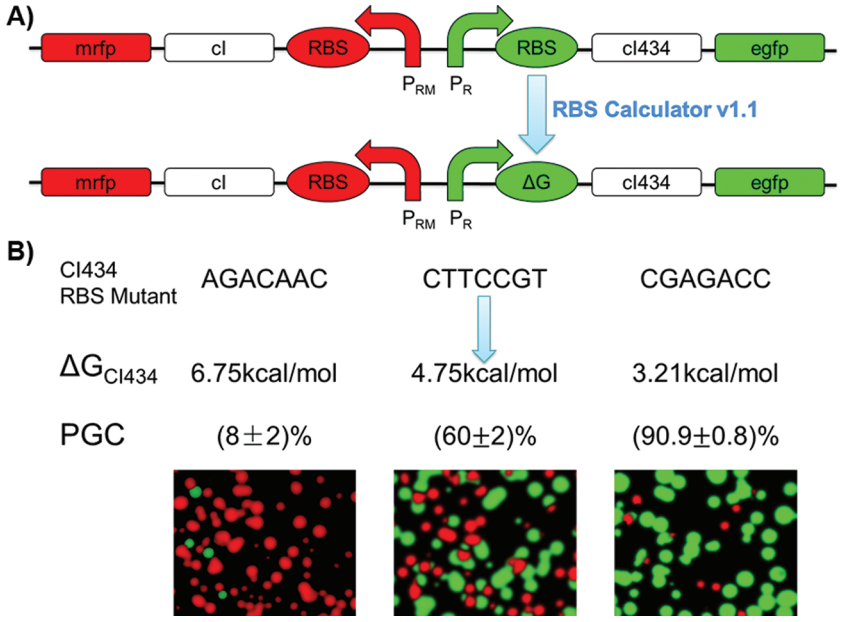

Figure 4. Tuning translation strength of cI434 by mutating its RBS sequence. (A) The RBS sequence prefixing cI434 could be converted into ΔG_{CI434}, the free energy change before and after translation initiation, by RBS calculator v1.1 (on the Web site of the Salis lab). (B) Images of cells carrying three representative toggle switch mutants (from left to right): C77, C68, and C42. Images are representatives of 5 independent recordings (Supplementary Figure S2), captured by fluorescence stereomicroscope and then merged. Each dot represents a colony.

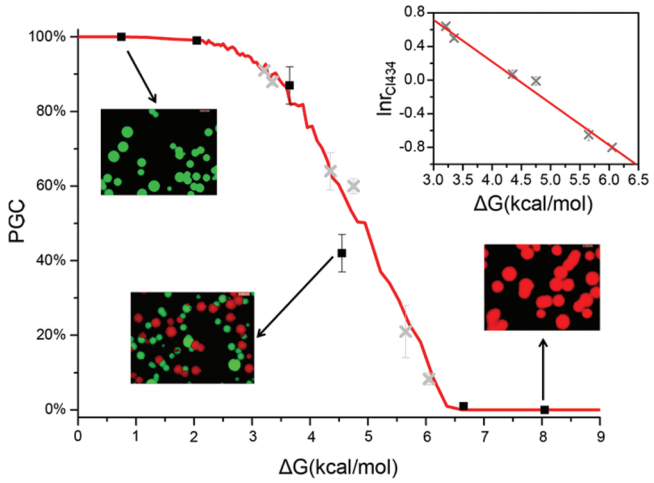

Figure 5. Establishment and verification of equivalence curve between ΔG_{CI434} and toggle switch bistability. With β and K_{CI434}, the equivalence curve was established (red solid line). Six RBS sequences predicted to exhibit different PGC values (0%, 0.5%, 58%, 86%, 99.4%, and 100%, respectively) with corresponding ΔG_{CI434} values (8.05, 6.65, 4.55, 3.65, 2.15, 0.75 kcal/mol) according to this equivalence curve were *in silico* designed and introduced into the toggle switch, resulting in cI434 RBS mutants F01, F02, F03, F04, F05, F06 (black squares). Experimentally measured PGC values of all six mutants are 0%, (1.0 ± 0.3)%, (42 ± 5)%, (87 ± 5)%, (99.1 + 0.4)%, and 100%, respectively. Inset: linear regression between ΔG_{CI434} and r_{CI434} to parametrize β and K_{CI434}. Six mutants, C01, C42, C68, C77, E07, and E06 (gray crosses in either figure), with different PGC values ((21 ± 7)%, (90.9 ± 0.8)%, (60 ± 2)%, (8 ± 2)%, (88 ± 1)%, and (64 ± 5)%, respectively) were utilized for parametrization. RBS sequences were converted into ΔG_{CI434} via RBS calculator, while r_{CI434} was numerically calculated from PGC on the basis of eq 2.

meet desired ΔG_{CI434} values. Therefore, RBS sequences that drive the genetic toggle switch with predetermined PGC values could be *in silico* predicted based on the equivalent curve deciphered in Figure 5. To confirm this, six RBS sequences expected to bring about distinct PGC values throughout the bistability transition interval (from PGC = 0% to PGC = 100%) were *in silico* designed (Table 1). To experimentally validate them, directed mutagenesis was conducted at the RBS region of cI434 on the original toggle switch to introduce designed RBS sequences. Reassuringly, PGC values of these rationally designed toggle switches precisely fit the prediction (Figure 5), indicating that the equivalence curve is very predictive.

With the deciphered equivalence, the process of derivation, optimization, and construction of our cI-cI434 genetic toggle switch can be accelerated for future study and application, such as fine-tuning the toggling threshold of the "memory module" in an adaptive learning gene circuit.[15] What's more, engineered microbial consortia have been widely expected to be promising in metabolic engineering, in which heavy metabolic burden is divided into separate "cell types".[25,26] A problem, however, still remains in regard to how to maintain the consortium homeostasis. Reasonably, toggle switches with predetermined bistability could act as a "population balancer" to balance the fractions of different phenotypes within a genetically homogeneous population.[27,28] If two pathways, for example, the ones to metabolize glucose and xylose, are controlled by a toggle switch, the fractions of *Escherichia coli* cells to metabolize only glucose and only xylose can be predetermined and robustly balanced.[29] When grown in co-culture, this strain can ferment sugars both efficiently and robustly.

Furthermore, this method can be generalized to genetic toggle switches made out of other different transcription repressors (Supplementary Discussion), facilitating the construction of biological circuits with increasing complexity. For instance, it has been proposed that a bank of genetic toggle switches with different bistability (i.e., different toggling thresholds) can act together as a "digital-to-analog converter" to discretize analog inputs into levels of digital output via sequential toggling.[15]

dx.doi.org/10.1021/sb300027y | *ACS Synth. Biol.* 2012, 1, 284–290

Moreover, it is difficult, if not impossible, to program many indispensable biological processes, such as bet-hedging and cell fate differentiation, without probabilistic genetic devices.[18,19,27,28] The rational design of probabilistic genetic devices, however, is more difficult than those carefully studied deterministic ones, because the function of a probabilistic device is not an input-output relation but a dynamic process featured by stochasticity. Our research here provides a promising approach to rationally designing probabilistic genetic devices by combining RBS design method with reflective stochastic model, i.e., establishing an equivalence between DNA sequence and device function.

In summary, in this report we have described a method to establish equivalence between the RBS DNA sequence of a toggle switch and its bistability. Since synthetic biology aims to program cells quickly and predictably,[1,4,15] model studies that are able to map a genetic device DNA sequence to its function will dramatically facilitate the development and application of synthetic biology for biotechnology use.[1,19] In this aspect, this research can serve as a good example.

METHODS

Translation Strength Prediction and RBS Sequence Designing. Translation strength of cI434 RBS was calculated using online RBS calculator v1.1: "Reverse Engineer RBS" (https://salis.psu.edu/software/reverse). RBS sequences meeting predetermined translation strength were designed using another module of online RBS calculator v1.1: Design: "RBS with Constraints" (https://salis.psu.edu/software/forward_withConstraints).

ASSOCIATED CONTENT

Supporting Information

Program code for simulation and parameter sensitivity analysis; detailed derivation of the mathematical model (ODE and stochastic model); supplementary figures, tables, methods, materials, and references. This material is available free of charge via the Internet at http://pubs.acs.org.

AUTHOR INFORMATION

Corresponding Author

*E-mail: qi@pku.edu.cn.

Author Contributions

‖These authors contributed equally to this work.

Author Contributions

Q.O. and H.Z. supervised the project. H.Z. and S.C. designed the research. S.C., J.F., and H.S. derived the mathematical model. S.C., H.Z., H.S., Y.G., and W.J. performed the experiment. S.C., H.Z., Y.G., and Z.Y. performed the fluorescence stereomicroscopy and image analysis. Q.O., S.C., H.Z., and H.S. analyzed the data and wrote the manuscript.

Notes

The authors declare no competing financial interest.

ACKNOWLEDGMENTS

This work is part of the project of the Peking University Team for the International Genetically Engineered Machine (iGEM) competition, 2011.The team received the Gold Medal Prize and Top Sixteen in the competition. We thank X. Liu, M. Tian, X. Zhang, and C. Lou for helpful discussion; H. Salis for kindly providing online RBS Calculator v1.1; J. Xi, R. Sun, and T. Mu for their assistance on experiment; and L. Liu for instrument support on imaging. This work was supported by the Teaching Center for Experimental Biology, the National Undergraduate Innovational Experimentation Program and funded by NSF of China (11074009, 10721463), NFFTBS of China (J1030623, J1103505, J1030310, J1103205) and MST of China (2009CB918500).

REFERENCES

(1) Khalil, A. S., and Collins, J. J. (2010) Synthetic biology: applications come of age. *Nat. Rev. Genet. 11*, 367−379.

(2) Gardner, T. S., Cantor, C. R., and Collins, J. J. (2000) Construction of a genetic toggle switch in *Escherichia coli*. *Nature 403*, 339−342.

(3) Elowitz, M. B., and Leibler, S. (2000) A synthetic oscillatory network of transcriptional regulators. *Nature 403*, 335−338.

(4) Purnick, P. E., and Weiss, R. (2009) The second wave of synthetic biology: from modules to systems. *Nat. Rev. Mol. Cell Biol. 10*, 410−422.

(5) Wang, X., Chen, X., and Yang, Y. (2012) Spatiotemporal control of gene expression by a light-switchable transgene system. *Nat. Methods 9*, 266−269.

(6) Levskaya, A., Weiner, O. D., Lim, W. A., and Voigt, C. A. (2009) Spatiotemporal control of cell signalling using a light-switchable protein interaction. *Nature 461*, 997−1001.

(7) Lou, C., Liu, X., Ni, M., Huang, Y., Huang, Q., Huang, L., Jiang, L., Lu, D., Wang, M., Liu, C., Chen, D., Chen, C., Chen, X., Yang, L., Ma, H., Chen, J., and Ouyang, Q. (2010) Synthesizing a novel genetic sequential logic circuit: a push-on push-off switch. *Mol. Syst. Biol. 6*, 350.

(8) Fung, E., Wong, W. W., Suen, J. K., Bulter, T., Lee, S. G., and Liao, J. C. (2005) A synthetic gene-metabolic oscillator. *Nature 435*, 118−122.

(9) Tigges, M., Marquez-Lago, T. T., Stelling, J., and Fussenegger, M. (2009) A tunable synthetic mammalian oscillator. *Nature 457*, 309−312.

(10) Danino, T., Mondragon-Palomino, O., Tsimring, L., and Hasty, J. (2010) A synchronized quorum of genetic clocks. *Nature 463*, 326−330.

(11) Prindle, A., Samayoa, P., Razinkov, I., Danino, T., Tsimring, L. S., and Hasty, J. (2012) A sensing array of radically coupled genetic "biopixels". *Nature 481*, 39−44.

(12) Anderson, J. C., Voigt, C. A., and Arkin, A. P. (2007) Environmental signal integration by a modular AND gate. *Mol. Syst. Biol. 3*, 133.

(13) Zhan, J., Ding, B., Ma, R., Ma, X., Su, X., Zhao, Y., Liu, Z., Wu, J., and Liu, H. (2010) Develop reusable and combinable designs for transcriptional logic gates. *Mol. Syst. Biol. 6*, 388.

(14) Wang, B., Kitney, R. I., Joly, N., and Buck, M. (2011) Engineering modular and orthogonal genetic logic gates for robust digital-like synthetic biology. *Nat. Commun. 2*, 508.

(15) Lu, T. K., Khalil, A. S., and Collins, J. J. (2009) Next-generation synthetic gene networks. *Nat. Biotechnol. 27*, 1139−1150.

(16) McKnight, S. L. (1986) Phage a: a genetic switch. *Science 233*, 1435−1436.

(17) Kussell, E., and Leibler, S. (2005) Phenotypic diversity, population growth, and information in fluctuating environments. *Science 309*, 2075−2078.

(18) Acar, M., Mettetal, J. T., and van Oudenaarden, A. (2008) Stochastic switching as a survival strategy in fluctuating environments. *Nat. Genet. 40*, 471−475.

(19) Clancy, K., and Voigt, C. A. (2010) Programming cells: towards an automated 'Genetic Compiler'. *Curr. Opin. Biotechnol. 21*, 572−581.

(20) Ellis, T., Wang, X., and Collins, J. J. (2009) Diversity-based, model-guided construction of synthetic gene networks with predicted functions. *Nat. Biotechnol. 27*, 465−471.

(21) Amit, R., Garcia, H. G., Phillips, R., and Fraser, S. E. (2011) Building enhancers from the ground up: a synthetic biology approach. *Cell 146*, 105−118.

(22) Carothers, J. M., Goler, J. A., Juminaga, D., and Keasling, J. D. (2011) Model-driven engineering of RNA devices to quantitatively program gene expression. *Science 334*, 1716−1719.
(23) Salis, H. M., Mirsky, E. A., and Voigt, C. A. (2009) Automated design of synthetic ribosome binding sites to control protein expression. *Nat. Biotechnol. 27*, 946−950.
(24) Canton, B., Labno, A., and Endy, D. (2008) Refinement and standardization of synthetic biological parts and devices. *Nat. Biotechnol. 26*, 787−793.
(25) Van Noorden, R. (2010) New year, new science. *Nature 463*, 12−13.
(26) Li, B., and You, L. (2011) Synthetic biology: Division of logic labour. *Nature 469*, 171−172.
(27) Eldar, A., and Elowitz, M. B. (2010) Functional roles for noise in genetic circuits. *Nature 467*, 167−173.
(28) Beaumont, H. J., Gallie, J., Kost, C., Ferguson, G. C., and Rainey, P. B. (2009) Experimental evolution of bet hedging. *Nature 462*, 90−93.
(29) Eiteman, M. A., Lee, S. A., and Altman, E. (2008) A co-fermentation strategy to consume sugar mixtures effectively. *J. Biol. Eng. 2*, 3.